Title
Phase-resolved frequency domain optical Doppler tomography

Authors
Wang, Lei
Wang, Yimin
Bachman, Mark
et al.

Publication Date
2004-07-01

DOI
10.1117/12.531421

Phase-resolved Frequency Domain Optical Doppler Tomography

Lei Wang [a,c], Yimin Wang[b,d], Mark Bachman [a,b,c], G.P. Li [a,b,c] and Zhongping Chen[*a,b,c,d]
[a] Department of Electrical Engineering and Computer Science
[b] Department of Biomedical Engineering
[c] UCI Integrated Nanosystems Research Facility
[d] Beckman Laser Institute
University of California, Irvine

ABSTRACT

We present a phase-resolved optical Doppler tomography (ODT) sys tem at 1310 nm using frequency domain method. Frequency domain phase-resolved ODT potentially allows for an increased longitudinal imaging range, signal-to-noise ratio and imaging acquisition rates, which can dramatically increase the measurable velocity dynamic range. A detailed derivation of phase-resolved frequency domain ODT and a measurement of flow through micro channel are presented. This technique can be used to quantify flow in integrated microfluidic devices in which complex three-dimensional structures and a wide velocity range are present.

Keywords: Optical Doppler Tomography, Flowmetry

INTRODUCTION

Optical Doppler tomography (ODT) is a noninvasive diagnostic technique for imaging sample structure and the cross sectional velocity distribution of moving scattering media [1]. Early ODT systems were unable to achieve simultaneously both high imaging speed and high velocity sensitivity. Phase-resolved ODT [2,3] provides information on flow velocity and variance in this velocity and several clinical applications of phase-resolved ODT have been reported [3]. We have also applied this noninvasive imaging technique to quantify micro flow and the result is comparable to those obtained by conventional testing method [4]. Recently, frequency domain optical coherence tomography (OCT) has attracted great attention due to its intrinsic advantage in signal-to-noise ratio. Several research groups have shown that frequency domain OCT has a signal-to-noise ratio approximately 20 dB higher than that of time domain OCT [9-11]. In addition, frequency domain OCT does not require any axial scanning and the imaging speed is determined by either the electronic detection system or the tuning rate of a tunable laser [5-15]. Because parallel data acquisition can be implemented in frequency domain, high speed A-line data rate is possible. This provides phase-resolved ODT a better signal-to-noise ratio since the phase noise (caused by

* zchen@laser.bli.uci.edu

Coherence Domain Optical Methods and Optical Coherence Tomography in Biomedicine VIII, edited by Valery V. Tuchin, Joseph A. Izatt, James G. Fujimoto, Proc. of SPIE Vol. 5316
(SPIE, Bellingham, WA, 2004) · 1605-7422/04/$15 · doi: 10.1117/12.531421

environmental vibration) will be minimized. Furthermore, higher A-line rate gives larger velocity dynamics range. Therefore, frequency domain ODT has advantages in applications where imaging speed and velocity dynamic range is important. In this paper, we report a frequency domain ODT system using phase-resolved algorithm to measure flow velocity. Frequency domain phase-resolved ODT is not only promising for high speed medical application but also important in quantifying integrated microfluidic devices where complex three-dimensional structures and a broad velocity range are present. We present phase-resolved ODT images using frequency domain method at 1310 nm. At this wavelength, bigger penetration depth is expected in biological sample.

PRINCIPLE

Frequency domain ODT system has the same configuration as frequency domain OCT, as shown in figure 1. The back-routed beams from the reference and sample arms are dispersed by a grating after exiting from fiber and incidence on a detector array.

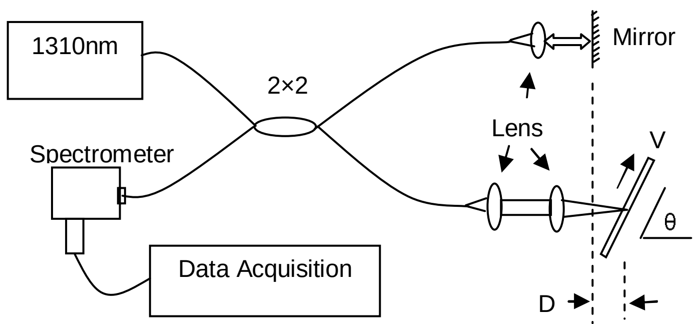

Fig. 1. Schematic of phase-resolved frequency domain ODT system. SLD, superluminescent diode; 2×2, fiber coupler; θ, Doppler angle; V, velocity of flow; D, path difference between sample and reference arms.

Light with different wavelength is detected by elements of a detector array. With an object in place in the sample arm, an interference spectrograph is generated at the detector array. The frequency domain representation of the interference pattern is described by equation (1), where $S(\omega)$ denotes the frequency distribution of light source, ω is the angular frequency of each wavelength component, R_r and R_s are reflection coefficient of the reference and sample arms, respectively, D is the path difference between the object and the reference mirror and c is the speed of light in free space. The initial phase difference is assumed to be zero.

$$I(\omega) = S(\omega)R_s + S(\omega)R_r + \sqrt{R_s R_r}\, S(\omega)\left[\exp(-j\frac{2D}{c}\omega) + \exp(+j\frac{2D}{c}\omega)\right] \qquad (1)$$

The spectrograph is modulated at a frequency determined by D. Using the inverse Fourier transform (IFT), a complex time domain reflective signal i(t) of the sample is obtained.

$$i(t) = R_s s(t) \otimes \delta(t) + R_r s(t) \otimes \delta(t) + 2\sqrt{R_r R_s}\, s(t) \otimes \left[\delta(t - 2D/c) + \delta(t + 2D/c)\right] \quad (2)$$

where s(t) is the IFT of S(ω), namely the wave package in time domain and ⊗ denotes convolution. The first two terms in equation (2) represent the DC component and the last term represents the corresponding relative time delay with respect to zero path difference. Due to the property of Fourier transform, a parasite image is also present [6,7,12]. Clearly, different optical path difference corresponds to different time delay.

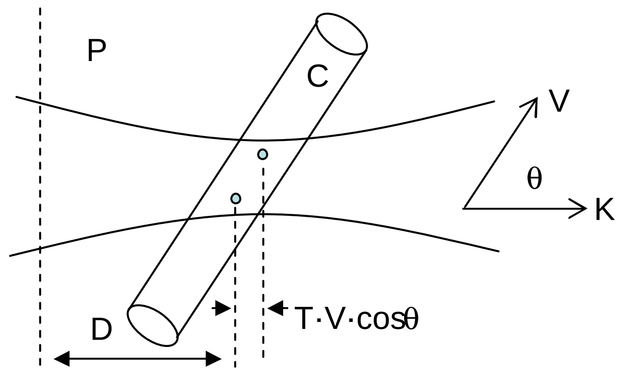

Fig. 2. Geometry of probe beam and single scatter flow through a micro tube. D, initial path difference; P, zero path difference plane; T, time elapsed; V, velocity of moving scatter, K, wave vector; C, micro channel

When considering the situation of a single moving scatter and assuming a homogeneous sample medium, as depicted in figure 2, the optical path difference is now equal to 2·(D+T·Vcosθ), where V is the velocity of the scatter, θ is the Doppler angle between the scatter direction of motion and ODT probe wave vector. The initial position of the moving scatter is D. According to modulation theorem, the corresponding time domain signal is a function of [2·(D+T·Vcosθ)/c]. Therefore, if the time delay between two sequential i(t) is known, we can calculate the velocity of the scatter by equation (3).

$$\frac{2Vc\text{os}\,\theta \cdot T}{c} = \tau_d \quad (3)$$

where T is the time interval between two sequential A-lines and τ_d is the optical time delay between two positions. However, it is difficult to determine the optical delay for each pixel directly. The optical time delay is extracted by comparing the average phase change between two sequential complex time domain reflective signals (i(t))

$$\tau_d = \frac{\overline{\Delta\psi}}{\overline{\omega}} = \frac{\overline{\Delta\psi}}{\omega_0} \quad (4)$$

where $\overline{\Delta\psi}$ is the average phase change, $\overline{\omega}$ is the average angular frequency of the light source and ω_0 is the center angular frequency if a Gaussian light source is assumed. Using the phase-resolved method, the phase change is determined by calculating the cross correlation function of two sequential complex spatial reflective signals [2-3], as described by equation (5).

$$\overline{\Delta\psi} = \tan^{-1}\left(\frac{\mathrm{Im}\left(\sum_{j=1}^{N}\left(i_j(t)\cdot i_{j+1}^{*}(t)\right)\right)}{\mathrm{Re}\left(\sum_{j=1}^{N}\left(i_j(t)\cdot i_{j+1}^{*}(t)\right)\right)}\right) \tag{5}$$

where Im and Re represent imaginary and real components of a complex, * denotes conjugate, N is the number of sequential data points to be averaged and j and j+1 are indices for sequential complex time domain reflective signals. From equations (3)-(5), the velocity can be evaluated as:

$$\frac{2Vc\,\mathrm{os}\,\theta\cdot T}{c} = \frac{\overline{\Delta\psi}}{\overline{\omega}} \tag{6}$$

The equation for calculating phase-resolved ODT maintains the same form in both the time domain and frequency domain, as expected. Due to the periodic property of the triangle function, a reliable velocity estimate is limited in a dynamic range within the time period of [-λ_0/2c, +λ_0/2c].

Fig. 3. Flowchart for phase-resolved frequency domain ODT signal processing

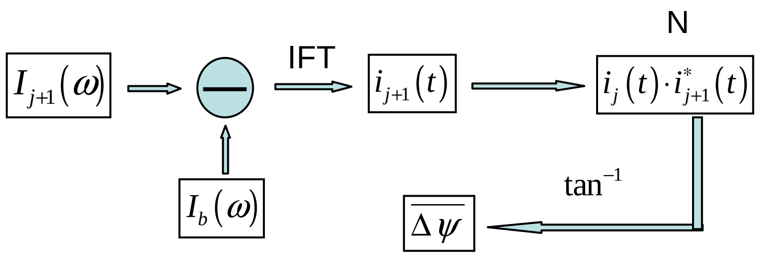

Figure 3 shows the signal processing scheme of our phase-resolved frequency domain ODT system. A background signal ($I_b(\omega)$) was recoded by blocking the sample arm, reducing considerably the DC component in time domain. After IFT of each A-line data, the time domain complex signal was correlated with the previous one. To increase the signal-to-noise ratio in the ODT images, 30 sequential A-lines were used for the calculation of the phase shift of each A-line pixel.

EXPERIMENTS

A super-luminescent diode centered at 1310 nm with a FWHM of 60 nm (corresponding to an axial resolution about 10 μm) was used as a broad band light source. It delivers a total power of 8 mW. The back routed beams were dispersed over a 1×512 InGaAs detector array of a 300 mm imaging spectrograph. The spectrometer had a spectral resolution of approximately 0.2 nm, corresponding to an imaging depth about 2.2 mm in free space. Although the exposure time was set to 300 μs the spectrum collection rate we achieved was approximately 80 Hz. The rate was limited by the data transfer rate from the detector controller to the computer. A spectrum of light from the reference arm was subtracted from each A-line spectrum to minimize the DC component. The sample arm was tilted at an angle of 84^{o} with respect to the flow direction, in order to get flow velocity projection. For a demonstration of frequency domain ODT, 2% Intralipid solution was used as working fluid. It was driven through a plastic tube (outer diameter: 780 μm; inner diameter:

260 μm) by a syringe pump at a fix pump rate of 0.3 μl/min. The whole experimental setup was mounted on a floating optical table to reduce the effects of environmental vibrations.

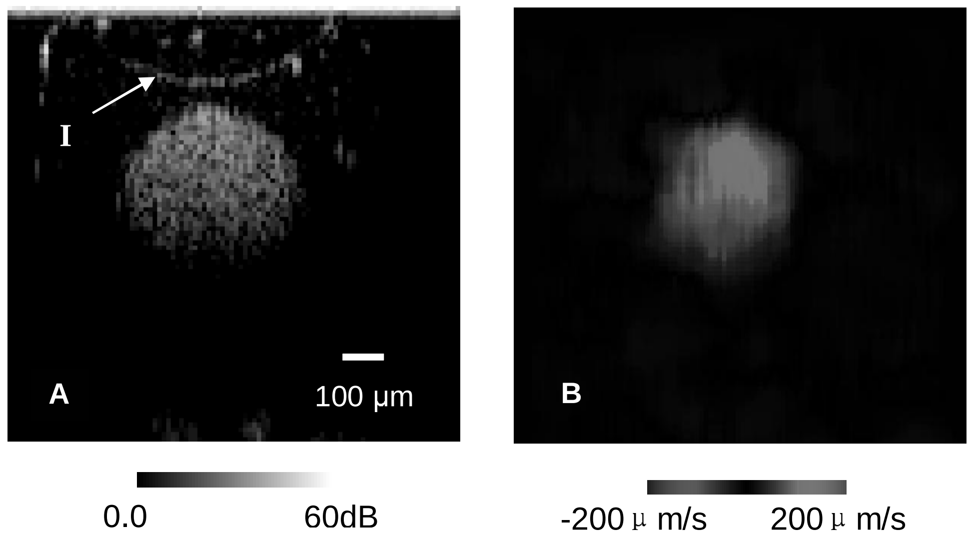

Fig. 4. Phase-resolved frequency domain OCT and ODT images. A, OCT image; B, ODT image; I, top outer surface; Image size, 1 mm × 0.9 mm

Figure 4 shows the structure and velocity images of a plastic tube obtained by frequency domain phase-resolved ODT. The horizontal scanning range was 1 mm, corresponding to 3000 A-lines. Every 30 A-lines were used to calculate the intensity and flow velocity of each A-line shown in figure 3. Fig. 4 A shows the structure image of the plastic tube with Intralipid. The plastic tube was placed close to the zero path difference position. The top outer surface (I) of the plastic tube was imaged backward because it lied on the other side of zero path difference position. Fig. 4 B is the velocity image of flowing Intralipid. The presence of different velocities (property of pressure driven flow) within the plastic tube was detected, as expected. The velocity was color coded, red and blue representing opposite flow directions.

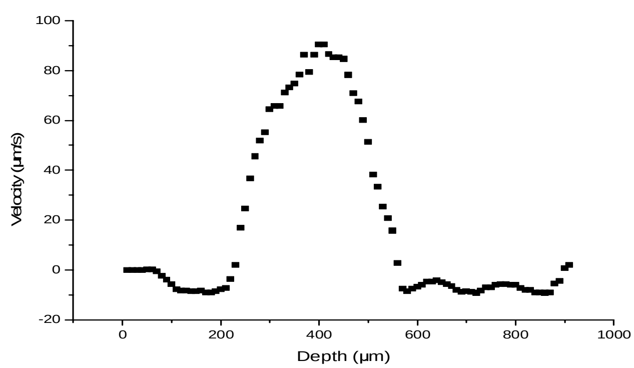

Fig. 5. Velocity profile measured by phase-resolved frequency domain ODT at the center of the conduit

A vertical cross section velocity profile at the center of the conduit is shown in figure 5, in which parabolic like velocity profile was observed. It indicates a laminar flow through the sample tube, as expected.

As described above, the imaging speed and velocity range are limited by the spectrum data transferring rate between detector controller and computer. However, high imaging speeds are possible if a high speed spectrometer is used. Furthermore, high data collection rate can reduce the phase noise and one does not need an air floated bench and tens averaging to get a good signal-to-noise ratio. An ultra-high speed spectrometer with 300 KHz spectral acquisition rates is currently available; if such a high speed spectrometer were used, a frame rate as high as 100 frames/s may be achieved with a velocity dynamic range of 1000 mm/s at a Doppler angle of 84^{o}. In addition, longitudinal imaging range can be increased with the use of a high-resolution spectrometer in conjunction with a large focal depth axicon lens [16]. This would allow for imaging of an object under a thick transparent media accessible, for example in three dimensional microfluidic networks.

CONCLUSION

In summary, we described the method of frequency domain phase-resolved ODT as a noninvasive flow diagnostic method. Since the imaging rate of the frequency domain method is not controlled by bus of a mechanical scanning device, this system is more flexible and can acquire images at faster rates. Furthermore, the velocity dynamic range can be increased considerably. Given the noninvasive nature of the measurement technique, high signal-to-noise ratio, high speed acquisition and simple hardware adjustment, frequency domain phase-resolved ODT may be prefered for real-time applications.

ACKNOWLEDHGEMENTS

We acknowledge the support of DARPA Bioflips (N66001-01-C8014), National Science Foundation (BES-86924), National Institutes of Health (EB-00293, NCL-91717, EB-F49620-00-0371) and the Beckman Laser Institute Endowment.

REFERENCES

1. Z. Chen, T. E. Milner, D. Dave, J. S. Nelson, "Optical Doppler tomographic imaging of f luid f low velocity in highly scat tering media", Opt. Lett., 22, 64, (1997)
2. Y. Zhao, Z. Chen, C. Saxer, S. Xiang, J.F. de Boer, J.S. Nelson, " Phase-resolved optical coherence tomography and optical Doppler tomography for imaging blood flow in human skin with fast scanning speed and high velocity sensitivity", Opt. Lett., 25, 114, (2000)
3. Y. Zhao, Z. Chen, C. Saxer, Q. Shen, S. Xiang, J.F. de Boer, J.S. Nelson, " Doppler standard deviation imaging for clinical monitoring of in vivo human skin blood flow", Opt. Lett., 25, 1358, (2000)
4. L. Wang, W. Xu, M. Bachman, G.P. Li, Z. Chen, " Imaging and quantifying of microflow by phase-resolved optical Doppler tomography", Proc. SPIE, 5345-26, (2004) (To be published).
5. A.F. Fercher, C.K. Hitzenberger, G. Kamp, S.Y. El-Zaiat, "Measurement of intraocular distances by backscattering spectral interferometry", " Optics Communication, 117, 43, (1995)
6. G. Hausler, M. W. Lindner, "Coherence radar and spectral radar- new tools for dermatological diagonosis", J. of Biomedical Optics, 3, 21, (1998)

7. M. Wojtkowski, R. Leitgeb, A. Kowalczyk, A. F. Fercher, " In vivo human retinal imaging by Fourier domain optical coherence tomography", J. of Biomedical Optics, 7, (2002)
8. S.H. Yun, G.J. Tearney, J.F. de Boer, N. Iftimia, B.E. Bouma, "High-speed optical frequency-domain imaging", Opt. Express, 11, 2953, (2003),
9. R. Leitgeb, C.K. Hitzenberger, A.F. Fercher, " Performance of Fourier domain vs. time domain optical coherence tomography", Opt. Express, 11, 889, (2003).
10. M.A. Choma, M.V. Sarunic, C. Yang, J.A. Izatt, "Sensitivity advantage of swept source and Fourier domain optical coherence tomography", Opt. Express, 11, 2183, (2003)
11. J.F. de Boer, B. Cense, B.H. Park, M.C. Pierce, G.J. Tearner, B. E. Bouma, "Improved signal-to-noise ratio in spectral-domain compared with time-domain optical coherence tomography", Opt. Lett., 28, 2067, (2003)
12. M. Wojtkowski, A. Kowalczyk, R. Leitgeb, A.F. Fercher, "Full range complex spectral optical coherence tomography technique in eye imaging", Opt. Lett., 27, 1415, (2002)
13. A.B. Vakhtin, K.A. Peterson, W.R. Wood, D.J. Kane, "Differential spectral interferometry: an imaging technique for biomedical applications", Opt. Lett., 28, 1332, (2003)
14. S.R. Chinn, E.A. Swanson, J.G. Fujimoto " Optical coherence tomography using a frequency-tunable optical source", Opt. Lett., 22, 340, (1997)
15. M. Wojtkowski, T. Bajraszewski, P. Targowski, A. Kowalczyk, "Real-time in vivo imaging by high-speed spectral optical coherence tomography", Opt. Lett., 28, 1745, (2003)
16. Z. Ding, H. Ren, Y. Zhao, J.S. Nelson, Z. Chen, "High-resolution optical coherence tomography over a large depth range with an axicon lens", Opt. Lett., 27, 243, (2002)